Density functional calculations on the geometric structure and properties of the 3d transition metal atom doped endohedral fullerene $M@C_{20}F_{20}$ (M = Sc–Ni)*

Tang Chun-Mei(唐春梅)[a)†], Zhu Wei-Hua(朱卫华)[a)], and Deng Kai-Ming(邓开明)[b)]

[a)] *College of Science, Hohai University, Nanjing* 210098, *China*

[b)] *Department of Applied Physics, Nanjing University of Science and Technology, Nanjing* 210094, *China*

(Received 2 March 2009; revised manuscript received 5 May 2009)

This paper uses the generalised gradient approximation based on density functional theory to analyse the geometric structure and properties of the 3d transition metal atom doped endohedral fullerene $M@C_{20}F_{20}$ (M = Sc–Ni). The geometric optimization shows that the cage centre is the most stable position for M, forming the structure named as $M@C_{20}F_{20}$-4. The inclusion energy, zero-point energy, and energy gap calculations tell us that $Ni@C_{20}F_{20}$-4 should be thermodynamically and kinetically stablest. $M@C_{20}F_{20}$-4 (M = Sc–Co) possesses high magnetic moments varied from 1 to 6 μ_B, while $Ni@C_{20}F_{20}$-4 is nonmagnetic. The Ni–C bond in $Ni@C_{20}F_{20}$-4 contains both the covalent and ionic characters.

Keywords: $M@C_{20}F_{20}$, transition metal, magnetic property, density functional

PACC: 3640B, 7500, 7115M

1. Introduction

The geometric structure of small carbon clusters is of basic interest to the understanding of fullerene formation.[1] The smallest possible fullerene C_{20} is extremely reactive due to its high curvature, however, it has been successfully synthesised.[2] Recently, dodecahedrane $C_{20}F_{20}$ has been isolated by the experiment.[3] Theortically, Zhang *et al.* have studied the properties of $X@C_{20}F_{20}$ ($X = H^-$, F^-, Cl^-, Br^-, H, He)[4] and $X@C_{20}F_{20}$ ($X = O^{2-}$, S^{2-}, Se^{2-}).[5] They pointed that these molecules are candidates for the electronic unit of nanomaterials. Up to now, lots of theoretical and experimental investigations are dedicated to explore the electronic and magnetic properties of transition metal atom (TMA) doped fullerenes.[6] For example, by endohedral-exohedral doping of C_{28} fullerene cage species such as $Ti@C_{28}H_4$ have been suggested to be stable and magnetic.[7] In addition, thermodynamic factors are discovered quite favorable for the formation of experimentally observed $Zr@C_{28}$ and $Sc@C_{28}$, which are calculated with different magnetism and ground states.[6] Kumar *et al.*[8,9] have doped different atoms into Si_nH_n(n = 10, 12, 16, 18, 20, 24, and 28), including TMA of Ti, V, Cr, Mn, Fe, Co, Zr, Ni, Nb, Mo, and W. They discovered that different TMA doped Si_nH_n have different stability, structural, electronic, and magnetic properties.

The interior diameter of $C_{20}F_{20}$ can be comparable to that of C_{28}. In addition, C_nF_n embodies similar bonding and structural properties to Si_nH_n.[8] Therefore, some interesting questions are then asked: whether the TMA could be trapped into $C_{20}F_{20}$? If they can, what is the most stable site for TMA in $C_{20}F_{20}$? What are the electronic and magnetic properties of these $C_{20}F_{20}$ derivatives? As we know, there have been no theoretical research published for $M@C_{20}F_{20}$ (M = Sc–Ni), therefore, we perform a comprehensive density functional study on the structure and electronic properties of them in this paper.

2. Computational details

All the calculations were performed by using the generalised gradient approximation based on density functional theory as implemented in the DMol program,[10] where the Becke-Lee-Yang–Parr correlation exchange functional(Becke[11] gradient exchange

*Project supported by the Research Starting Foundation of Hohai University (Grant No. 2084/40801130), the Natural Science Foundation of Hohai University (Grant Nos. 2008431211 and 2008430311), the Excellent Innovation Personal Support Plan of Hohai University, the Basic Scientific Research Foundation of National Central, and the Special Foundation of the Natural Natural Science (Grant No. 10947132).

†Corresponding author. E-mail: tcmnj@163.com

© 2010 Chinese Physical Society and IOP Publishing Ltd

functional combined with Lee, Yang and Parr[12] correlation functional) is chosen together with the DNP basis set(double-numerical basis functions together with polarization functions). The electronic structure was obtained by solving the Kohn–Sham[13] equations self-consistently under the spin unrestricted condition. Mulliken population analysis was made to obtain both the charge and net spin populations on each atom. Self-consistent field procedures are done with a convergence criterion of 10^{-6} a.u. on the energy and electron density. Geometrical optimizations were performed by using the Broyden–Fletcher–Goldfarb–Shanno algorithm[13] with a convergence criterion of 10^{-3} a.u. on the displacement and 10^{-5} a.u. on the energy.

3. Results and discussions

3.1. The stability

All the pentagons are equal in the dodecahedrane $C_{20}F_{20}$, therefore, only three unequal sites near the pentagon and the cage centre are chosen to situate the TMA to form four different isomers, respectively named as $M@C_{20}F_{20}$-1(M is near the pentagon centre), $M@C_{20}F_{20}$-2 (M is near the centre of the [5, 5] bond), $M@C_{20}F_{20}$-3 (M is near the vertex of three pentagons), and $M@C_{20}F_{20}$-4 (M is in the cage centre), whose initial geometric structures are shown in Fig. 1(a). The M, situated at about 0.5 Å off-centre in $M@C_{20}F_{20}$-1, $M@C_{20}F_{20}$-2, and $M@C_{20}F_{20}$-3, are all drawn back to the cage centre (within 0.02 Å tolerance) without distortion of the cage (the cage is still I_h symmetric within 0.02 Å tolerance). However, the M in $M@C_{20}F_{20}$-4 is still situated at the cage centre. Therefore, the cage centre is the most stable position for M. We mainly study the detailed properties of $M@C_{20}F_{20}$-4 (M = Sc–Ni) in the following.

Table 1 presents the inclusion energies ($\Delta E_{\rm inc}$), the zero-point energies (ZPE), and the energy gaps ($E_{\rm g}$) between the highest occupied molecular orbital (HOMO) and the lowest unoccupied molecular orbital (LUMO) of the optimized $M@C_{20}F_{20}$-4 (M = Sc–Ni). The $\Delta E_{\rm inc}$ is defined as the energy difference between $Ni@C_{20}F_{20}$ and the sum of the isolated $C_{20}F_{20}$ and Ni.[14] The higher positive $\Delta E_{\rm inc}$ leads to the greater thermodynamic stability of the resultant.[15] The EGs of all the considered structures are often correlated with the kinetic stabilities.[16] It is known from Table 1 that the $\Delta E_{\rm inc}$ of $M@C_{20}F_{20}$-4 (M = Sc–Ni) are all positive and larger than those of the cage $C_{20}H_{20}$ with N, C^-, Si^-, O^+, Ne, Ar, Be, and Mg situated at the cage centre,[14,17] indicating the formations of $M@C_{20}F_{20}$-4 (M = Sc–Ni) are all exothermic and energetically favored. We can notice that $Ni@C_{20}F_{20}$-4 has the largest $\Delta E_{\rm inc}$ and ZPE, showing that it is the thermodynamically stablest. The $E_{\rm g}$ of $Ni@C_{20}F_{20}$-4 is the largest of all, implying that it is more kinetically stable than others. Therefore, $Ni@C_{20}F_{20}$-4 should be thermodynamically and kinetically stablest.

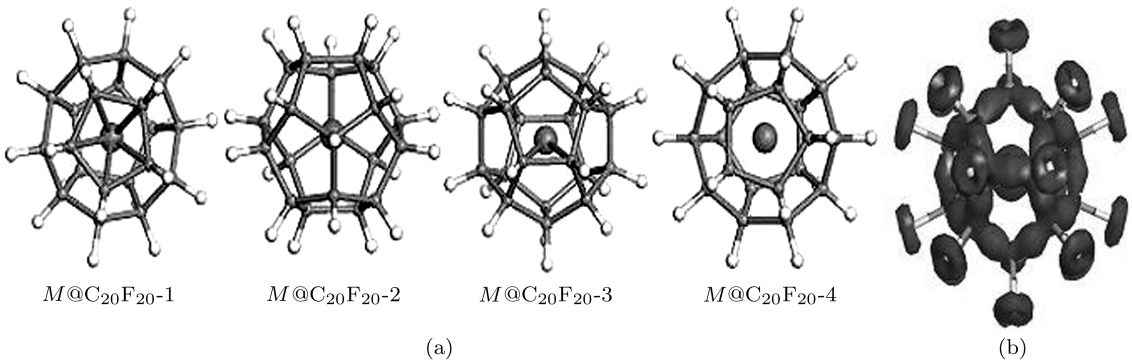


Fig. 1. (a) The initial geometric structures of four $M@C_{20}F_{20}$ isomers. (b) The difference charge density of $Ni@C_{20}F_{20}$-4.

Table 1. The $\Delta E_{\rm inc}$, ZEP, and $E_{\rm g}$ of the optimized $M@C_{20}F_{20}$-4 (M = Sc–Ni)(eV).

$M@C_{20}F_{20}$-4	Sc	Ti	V	Cr	Mn	Fe	Co	Ni
$\Delta E_{\rm inc}$	8.58	7.97	8.05	7.12	7.50	7.88	7.60	8.78
ZPE	4.37	4.41	4.47	4.43	4.46	4.42	4.20	5.67
$E_{\rm g}$	0.23	0.38	0.60	0.58	0.42	0.73	0.43	1.38

3.2. The magnetism

Based on the optimised geometries, the magnetic properties of the M@$C_{20}F_{20}$ (M = Sc–Ni) clusters were evaluated via the Mulliken charge population analysis and the results are presented in Table 2. For M@$C_{20}F_{20}$-4 (M = Sc–Co), the total magnetic moments of them are mainly located at M site when they are compared with the local spin magnetic moment of M. The charges of the 3d states of M are 1.407 e, 2.685 e, 3.909 e, 4.356 e, 2.650 e, 1.806 e, 0.946 e and 0 e. According to the Hund's rule, the magnetic moments of the 3d states should be 1.407 μ_B, 2.685 μ_B, 3.909 μ_B, 4.356 μ_B, 2.650 μ_B, 1.806 μ_B, 0.946 μ_B, and 0 μ_B. Therefore, the origin of the M_{TMA} mainly come from the 3d state. Due to the charge transfer between the carbon atoms and M and the internal charge transfer between 4s, 3d, 4p, and other states of M, M@$C_{20}F_{20}$-4 (M = Sc–Co) has high magnetic moment varied from 1 to 6 μ_B. Thus, we can come to the conclusion that M@$C_{20}F_{20}$-4 (TM = Sc–Co) possesses tunable magnetic properties and has potential utility in new nanomaterials. As to Ni@$C_{20}F_{20}$-4, the 3d, 4s, and 4p states of Ni have 9.396 e, 0.092 e, and 0.161 e respectively, indicating that its 4s state loses 1.504 e, while the 4p and 3d states capture 1.396 e and 0.161 e respectively. However, Ni captures about 0.092 e from the C atoms, which is too small to be ignored. Ni@$C_{20}F_{20}$-4 has a closed shell electronic structure and is nonmagnetic, similar to some Ni-doped clusters but different from other TMA doped clusters.[9] From the analysis above, Ni@$C_{20}F_{20}$-4 is discovered to have the stablest and embody nonmagnetic character, therefore, other properties of Ni@$C_{20}F_{20}$-4 will be discussed in detail as follows.

Table 2. The charge and the magnetic moments of the M@$C_{20}F_{20}$-4 (M = Sc–Ni) clusters. C_{TMA} means the charge of the M; M_{total} and M_{TMA} are the magnetic moments of the M@$C_{20}F_{20}$-4 clusters and the M, respectively; C_{3d}, C_{4s}, C_{4p} are the charge of the 3d, 4s, 4p states of the M respectively; and M_{3d}, M_{4s}, M_{4p}, M_{atom} are the magnetic moments of the 3d, 4s, 4p states of the M and the atom, respectively.

	M_{TMA}/μ_B	C_{TMA}/(e)	M_{total}/μ_B	C_{3d}/(e)	M_{3d}/μ_B	C_{4s}/(e)	M_{4s}/μ_B	C_{4p}/(e)	M_{4p}/μ_B
Sc@$C_{20}F_{20}$-4	1.683	0.446	3	1.790	1.407	0.695	0.260	0.000	0.000
Ti@$C_{20}F_{20}$-4	2.848	0.183	4	3.080	2.685	0.562	0.103	0.102	0.056
V@$C_{20}F_{20}$-4	3.995	0.037	5	4.282	3.909	0.483	0.013	0.120	0.074
Cr@$C_{20}F_{20}$-4	4.792	0.137	6	4.738	4.356	0.860	0.350	0.257	0.096
Mn@$C_{20}F_{20}$-4	2.698	–0.111	3	6.330	2.650	0.532	0.008	0.198	0.044
Fe@$C_{20}F_{20}$-4	1.834	–0.054	2	7.300	1.806	0.526	0.006	0.189	0.024
Co@$C_{20}F_{20}$-4	0.958	0.196	1	8.358	0.946	0.558	0.001	0.243	0.013
Ni@$C_{20}F_{20}$-4	0.000	–0.092	0	9.396	0.000	0.496	0.000	0.161	0.000

3.3. The electronic properties of Ni@$C_{20}F_{20}$-4

Figure 2 shows the energy levels of $C_{20}F_{20}$ and Ni@$C_{20}F_{20}$-4. The molecular orbitals whose energies agree with each other within a difference of 0.05 eV are regarded as degenerate, and the length of the horizontal bar shows the orbital degeneracy. The broken lines stand for the unoccupied orbitals and the solid lines stand for the occupied orbitals. We define the Fermi level as halfway between HOMO and LUMO. It is seen from Fig. 2 that the LUMO of $C_{20}F_{20}$ is near the LUMO of Ni@$C_{20}F_{20}$-4, the HOMO of $C_{20}F_{20}$ is close to the HOMO-1 of Ni@$C_{20}F_{20}$-4. Moreover, the degeneracies of the energy levels above the LUMO of $C_{20}F_{20}$ are as same as those of the energy levels above the LUMO of Ni@$C_{20}F_{20}$-4, while the energy levels below the HOMO of $C_{20}F_{20}$ have the same degeneracies as those of the energy levels below the HOMO-1 of Ni@$C_{20}F_{20}$-4. All the energy levels of $C_{20}F_{20}$ shift downwards when Ni is doped into the cage centre, forming an E_g about 2.55 eV smaller than that of $C_{20}F_{20}$, indicating that the doped Ni does not bring much influence to the deep energy levels. In order to know whether the HOMO of Ni@$C_{20}F_{20}$-4 comes from Ni or the $C_{20}F_{20}$ cage, the probability isodensities of HOMO and HOMO-1 of Ni@$C_{20}F_{20}$-4 are presented in Fig. 2. Obviously, the HOMO almost distributes on the Ni atom, while the LUMO-1 is dominated by the cage. Therefore, the HOMO of Ni@$C_{20}F_{20}$-4 comes from Ni, the levels below the HOMO mainly contain the carbon and fluorin characters.

As we know, it makes sense to discuss the difference charge density distribution in Fig. 1(b), obtained from the total density with the density of the isolated atoms subtracted,[18] because the bond nature can be determined from it.[19] Obviously, it is observed from Fig. 1(b) that there are some difference charge density accumulations between Ni and $C_{20}F_{20}$. Therefore, the interaction of Ni with $C_{20}F_{20}$ presents a small covalent character and, due to the small charge transfer found and the shortest Ni–C bond length (2.23 Å), longer than the sum of the radii of Ni and C (1.92 Å), it may also present small ionic character. Therefore, the Ni–C bond contains both the covalent and ionic characters, similar to that of the Ni–C bond in Ni@C_{60}.[20]

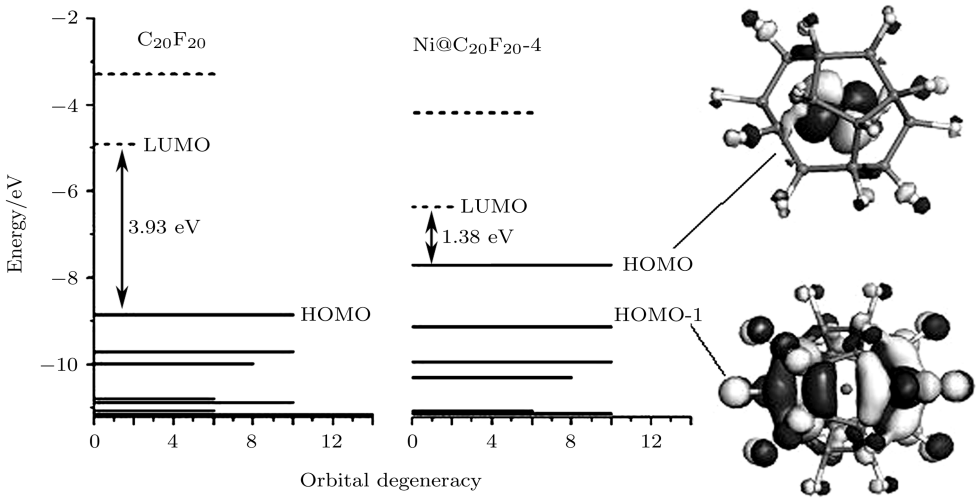


Fig. 2. The energy levels of $C_{20}F_{20}$ and Ni@$C_{20}F_{20}$-4, and the probability isodensities of HOMO and HOMO-1 of Ni@$C_{20}F_{20}$-4.

4. Conclusion

The geometric optimization shows that the cage centre is the most stable position for the M atom, forming the structure named as M@$C_{20}F_{20}$-4. The Ni@$C_{20}F_{20}$-4 should be thermodynamically and kinetically stablest of all. The M@$C_{20}F_{20}$-4 (M = Sc–Co) possesses high magnetic moments varied from 1 to 6 μ_B, while Ni@$C_{20}F_{20}$-4 is nonmagnetic. The Ni–C bond in Ni@$C_{20}F_{20}$-4 contains both the covalent and ionic characters.

References

[1] Curl R F 1993 *Philos. Trans. R. Soc. London* **343** 19
[2] Prinzbach H, Weiler A, Landenberger P, Wahl F, Wörth J L, Scott T, Gelmont M, Olevano D and Issendorff B V 2000 *Nature* (London) **407** 60
[3] Prinzbach H and Weber K 1995 *Angew. Chem. Int. Ed. Engl.* **33** 2239
[4] Zhang C Y, Wu H S and Jiao H J 2007 *J. Mol. Model.* **13** 499
[5] Zhang C Y, Wu H S and Jiao X 2007 *J. Mole. Struct: Theochem.* **71** 815
[6] Ordejòn P, Artacho E and Soler J M 1996 *Phys. Rev.* B **53** R10441
[7] Guo T, Smalley R E and Scuseria G E 1993 *J. Chem. Phys.* **99** 352
[8] Kumar V and Kawazoe Y 2003 *Phys. Rev. Lett.* **90** 055502
[9] Kumar V and Kawazoe Y 2007 *Phys. Rev.* B **75** 155425
[10] Deller B 1990 *J. Chem. Phys.* **92** 508
[11] Becke A D 1988 *J. Am. Chem. Phys.* **88** 1053
[12] Perdew J P and Wang Y 1992 *Phys. Rev.* B **45** 13244
[13] Jimenez V H A, Tamariz J and Cross R J 2001 *J. Phys. Chem.* A **105** 1315
[14] Chen Z F, Jiao H J, Moran D, Hirsch A, Thiel W and Schleyer P V 2003 *J. Phys. Chem.* A **107** 2075
[15] Lu G L, Yuan Y B, Deng K M, Wu H P, Yang J L and Wang X 2006 *Chem. Phys. Lett.* **424** 142
[16] Aihara J I 1999 *Theor. Chem. Acc.* **102** 134
[17] Moran D, Stahl F, Jemmis E D, Schaefer H F and Schleyer P R 2002 *J. Phys. Chem.* A **106** 5144
[18] Hossain M Z, Kato H S and Kawai M 2005 *J. Am. Chem. Soc.* **127** 15030
[19] Shaltaf R, Mete E and Eilialtroglu S 2005 *Phys. Rev.* B **72** 205415
[20] Salas R E E and Valladares A A 2008 *J. Mole. Struct: Theochem.* **869** 1